AIP Advances

Room-temperature ferromagnetic transitions and the temperature dependence of magnetic behaviors in FeCoNiCr-based high-entropy alloys

Cite as: AIP Advances **8**, 056412 (2018); https://doi.org/10.1063/1.5007073
Submitted: 29 September 2017 • Accepted: 03 November 2017 • Published Online: 21 December 2017

Suok-Min Na, Jin-Hyeong Yoo, Paul K. Lambert, et al.

AIP ADVANCES **8**, 056412 (2018)

Room-temperature ferromagnetic transitions and the temperature dependence of magnetic behaviors in FeCoNiCr-based high-entropy alloys

Suok-Min Na,[1,a] Jin-Hyeong Yoo,[2] Paul K. Lambert,[2] and Nicholas J. Jones[2]
[1]*Spectrum Technology Group, Inc., Gaithersburg, MD 20877, USA*
[2]*Physical Metallurgy and Fire Protection Branch, Naval Surface Warfare Center, Carderock Division, West Bethesda, MD 20817, USA*

(Presented 8 November 2017; received 29 September 2017; accepted 3 November 2017; published online 21 December 2017)

High-entropy alloys (HEAs) containing multiple principle alloying elements exhibit unique properties so they are currently receiving great attention for developing innovative alloy designs. In FeCoNi-based HEAs, magnetic behaviors strongly depend on the addition of alloying elements, usually accompanied by structural changes. In this work, the effect of non-magnetic components on the ferromagnetic transition and magnetic behaviors in equiatomic FeCoNiCrX (X=Al, Ga, Mn and Sn) HEAs was investigated. Alloy ingots of nominal compositions of HEAs were prepared by arc melting and the button ingots were cut into discs for magnetic measurements as functions of magnetic field and temperature. The HEAs of FeCoNiCrMn and FeCoNiCrSn show typical paramagnetic behaviors, composed of solid solution FCC matrix, while the additions of Ga and Al in FeCoNiCr exhibit ferromagnetic behaviors, along with the coexistence of FCC and BCC phases due to spinodal decomposition. The partial phase transition in both HEAs with the additions of Ga and Al would enhance ferromagnetic properties due to the addition of the BCC phase. The saturation magnetization for the base alloy FeCoNiCr is 0.5 emu/g at the applied field of 20 kOe (T_C = 104 K). For the HEAs of FeCoNiCrGa and FeCoNiCrAl, the saturation magnetization significantly increased to 38 emu/g (T_C = 703 K) and 25 emu/g (T_C = 277 K), respectively. To evaluate the possibility of solid solution FCC and BCC phases in FeCoNiCr-type HEAs, we introduced a parameter of valence electron concentration (*VEC*). The proposed rule for solid solution formation by the *VEC* was matched with FeCoNiCr-type HEAs. https://doi.org/10.1063/1.5007073

I. INTRODUCTION

High-entropy alloys (HEAs) contain multiple principle alloying elements with nearly equiatomic composition, unlike conventional alloys which are based on one major element and several minor elements such as iron in steels.[1] The HEA experimental data drawn from more than 400 different designed alloys were reported to have unique physical properties.[2] These properties are directly related to the so-called four core effects: high entropy of mixing instead of the formation of complex phases and/or intermetallic compounds, sluggish diffusion, severe lattice distortion, and cocktail effects.[1,2] The cocktail effect refers to the enhancement in various properties through elemental additions or replacements and provides useful guidelines for exploring structure-magnetic property correlations in HEAs. The effects of Al, Sn and Nb additions to single-phase HEAs were most widely studied.[2,3] Magnetic HEAs have recently drawn attention, with hopes of developing innovative alloy designs for

[a]Corresponding author: Suok-Min Na, e-mail address: nsmv2k@gmail.com

soft magnetic materials, rare-earth-free permanent magnets, magnetic refrigeration materials based on the magnetocaloric effect and so on.[4]

The starting base alloy is an equiatomic FeCoNi composed of ferromagnetic elements only, exhibiting a high saturation magnetization value (M_S) of 161 emu/g that is similar to that of Co (M_S=159.5 emu/g) in our preliminary work. The crystal structure of FeCoNi with a simple face-centered cubic (FCC) phase retained after adding an antiferromagnetic element such as Mn and Cr to form the quaternary alloys, but the magnetic behaviors were different between FeCoNiMn and FeCoNiCr alloys.[5] FeCoNiMn alloy still showed a ferromagnetic hysteresis loop with a low M_S of 18.14 emu/g, while FeCoNiCr alloy fully turned into paramagnetic state at room temperature (RT). And it was found that the dramatic phase transition from FCC to body-centered cubic (BCC) structure leads to the significant enhancement of ferromagnetic properties by adding non-magnetic alloying elements such as Al, Ga and Sn to FeCoNiMn alloy.[5,6] In contrast to the addition of Mn, ferromagnetic FeCoNi alloys can become paramagnetic at RT by adding Cr or CrMn in an equiatomic composition, resulting in a significant reduction of the Curie temperatures (T_C) from 868 K to 156 K for the Cr addition and 23 K for the CrMn addition in simulation.[7] It was observed that the T_C increased to 355 K and 640 K when Al and Ge, respectively, were added to the FeCoNiCr alloy.[8] The change in T_C was accompanied by structural decomposition into a mixture of FCC and BCC solid solution phases. In this work, the effect of non-magnetic components on the ferromagnetic transition and magnetic behaviors of equiatomic FeCoNiCrX (X=Al, Ga, Mn and Sn) HEAs was investigated. We also present the results of the FeCoNi and FeCoNiCr alloys as the base composition response.

II. EXPERIMENTAL PROCEDURES

Alloy ingots of nominal equiatomic compositions of FeCoNi, FeCoNiCr and FeCoNiCrX (X=Al, Ga, Mn and Sn) HEAs, were prepared by arc melting under a high purity argon atmosphere. The purity of elements was higher than 99.99 atomic percent (at.%). The arc-melted buttons were remelted five times and flipped each time to ensure that they were homogeneous in composition. The mass of each button ingot was approximately 60 grams. The button ingots were subsequently annealed at a temperature of 1000 °C for 48 hours to improve the local chemical homogeneity. Slices with thicknesses of ~0.38 mm were cut from each button. From these slices, discs with a diameter of 8.10 mm were extracted for microstructural analysis and room temperature magnetic measurements. Square pieces with dimensions less than 2 mm × 2 mm were cut for low temperature measurements from FeCoNiCrX (X=Al, Ga and Mn) HEAs and a disc sample with a diameter of 4.0 mm was cut from a slice of FeCoNiCrGa HEA for high temperature measurements.

Magnetic field dependence of magnetization (*M-H*) was measured at RT using a vibrating sample magnetometer (VSM) under applied magnetic fields up to ±20 kOe and temperature dependence of magnetization (*M-T*) was measured in the both temperature ranges of 2 – 380 K using a Quantum Design Magnetic Property Measurement System (MPMS XL) and 303 – 1123 K using a high temperature oven attached to the VSM.

To analyze structural properties, the fine polished samples were placed in a Scanning Electron Microscope (SEM, Hitachi SU6600) to get Electron Backscattered Diffraction (EBSD) patterns. Energy dispersive x-ray spectroscopy (EDS, EDAX Genesis) was used for collecting compositional data.

III. RESULTS AND DISCUSSION

The significant enhancement of ferromagnetic properties was observed in HEAs with equiatomic additions of Al, Ga and Sn in FeCoNiMn.[5] This enhancement was caused by a phase change from FCC in FeCoNiMn to BCC/B2 structures, producing an increase in saturation magnetization (M_S) and Curie temperature (T_C). The quaternary FeCoNiCr alloy also exhibited the FCC structure like FeCoNiMn although elemental Cr and Mn have a BCC structure with antiferromagnetism. Figure 1 shows XRD patterns for the FeCoNiCrX HEAs (X=Al, Ga, Mn and Sn). FeCoNiCrMn shows exactly the same XRD pattern as the FeCoNiCr, and FeCoNiCrSn contains Co-Sn intermetallic compounds

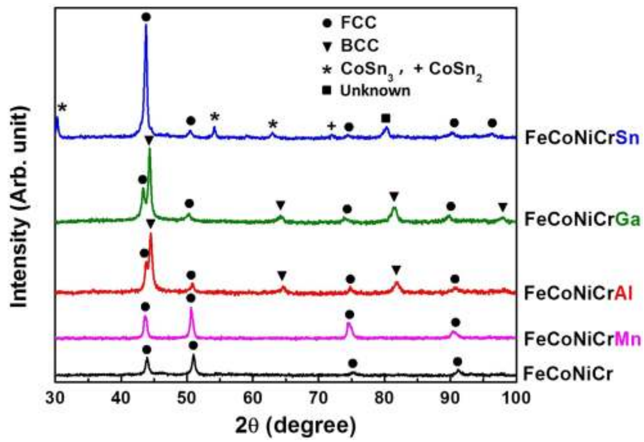

FIG. 1. X-ray diffraction (XRD) patterns of the FeCoNiCr and FeCoNiCrX (X=Al, Ga, Mn and Sn) HEAs.

within the FCC matrix, while FeCoNiCrAl and FeCoNiCrGa HEAs show the coexistence of simple FCC and BCC phases as shown in Table I.

Two millimeter-sized islands were found on the slice of FeCoNiCrGa HEA and were cut into discs noted as 'A' and 'B' in Fig. 2(a). Both discs include the matrix and an island. Figure 2(b) shows one of the islands with a length of several millimeters, which is located at the center of the slice. The EBSD phase map and EDS maps for all elements from the selected area across the interface between matrix and island are shown in Fig. 2(c)–(h). Those maps reveal a typical dendrite microstructure composed of BCC and FCC phases in the matrix[9,10] and an Fe-rich BCC phase corresponding to the island. The dendrites have a modulated plate structure associated with spinodal decomposition.[1,11] The elements of Ni and Ga are enriched in the matrix BCC phase, while Fe, Co and Cr are dominant in the FCC phase. Elemental Fe (93 at.%) is predominantly decomposed to the location of the island via a spinodal reaction as well, but the clustering is not understood so far. The microstructure of FeCoNiCrAl is also similar with that of FeCoNiCrGa, exhibiting a uniform distribution of dendritic structures and no clustering (not shown in this paper), and the trend in preferential decomposition is also similar to that of FeCoNiCrGa. The EDS compositional analysis for each phase in the dendritic matrix is summarized in Table II, including the results of FeCoNiCrMn. The actual composition of single FCC FeCoNiCrMn is closely approaching the nominal composition of 20 at.% for each element, with deviations within ±1 at.%.

In order to investigate the correlation between magnetic and structural properties, magnetic hysteresis loops and temperature dependence of magnetization were measured in FeCoNiCrX HEAs as shown in Fig. 3. The paramagnetic property in the FeCoNiCr alloy (labelled as FCNC in the insertion of Fig. 3(a)) with an FCC solid solution was dramatically changed to ferromagnetism by adding Ga or Al although both elements are non-magnetic components, while the addition of Mn or Sn retained the paramagnetic behavior of FeCoNiCr. Even though the addition of Ga or Al restored the magnetic condition to ferromagnetism originating in FeCoNi, the saturation magnetization was

TABLE I. A summary of structural changes in HEAs of FeCoNiMn-type and FeCoNiCr-type.

FeCoNiMn-type[a]	Structures	Magnetic state	FeCoNiCr-type[b]	Structures	Magnetic state
FeCoNiMn	FCC	ferro	FeCoNiCr	FCC	para
FeCoNiMnAl	BCC/B2	ferro	FeCoNiCrAl	BCC/FCC	ferro
FeCoNiMnGa	BCC/FCC	ferro	FeCoNiCrGa	BCC/FCC	ferro
FeCoNiMnCr	FCC	para	FeCoNiCrMn	FCC	para
FeCoNiMnSn	BCC/Co_2MnSn	ferro	FeCoNiCrSn	FCC/$CoSn_2$/$CoSn_3$	para

[a]Results from the Ref. 5,

[b]Our results.

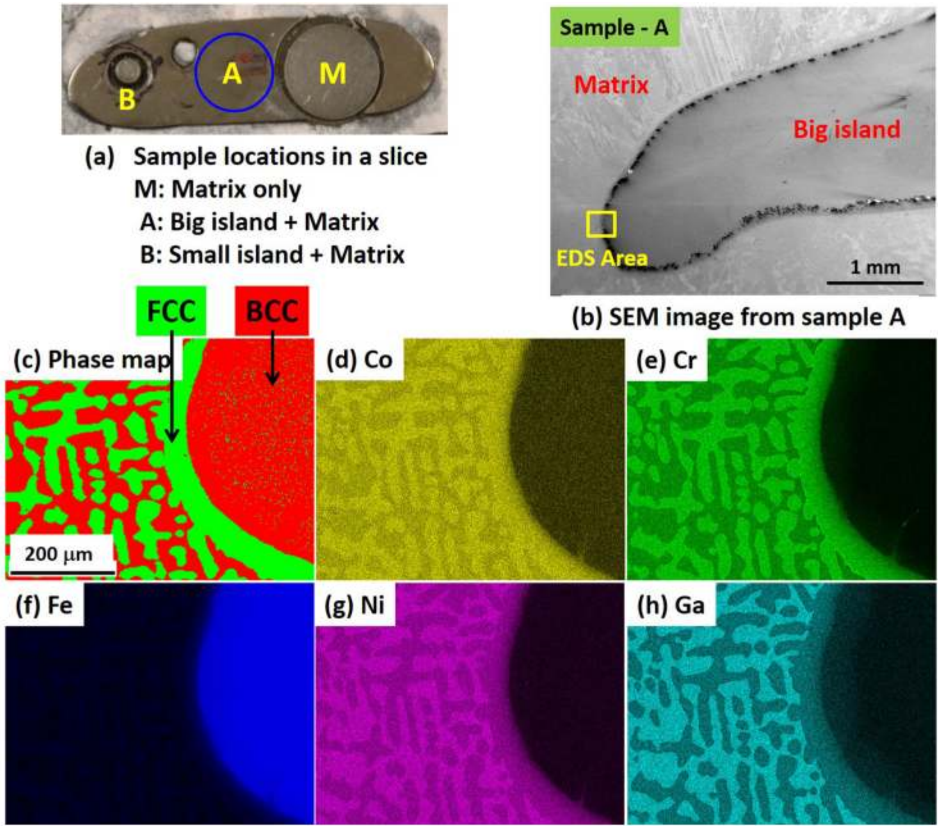

FIG. 2. Microstructural and compositional analysis of FeCoNiCrGa HEA: (a) a photo of a slice of the arc-melted button and disc sample locations, (b) an SEM image of sample 'A' across the interface between the matrix and big island, (c) phase map obtained from the EBSD scan of the selected area of (b), (d)-(h) EDS maps of Co, Cr, Fe, Ni, Ga elements, respectively, corresponding to the area of the phase map.

significantly reduced to 38 emu/g (Ga addition) and 25 emu/g (Al addition) from 161 emu/g for FeCoNi. It is straightforward to assume that the saturation magnetization will reduce with an increase in the amount of non-magnetic elements to the FeCoNi alloy. And, considering the effect of Ga and Al on the partial phase change, it is reasonable to assume that the phase change from FCC to BCC is strongly correlated to the RT magnetic transition. Interestingly, in the case of a full phase transition from FCC to BCC/B2, the saturation magnetization increased back to 148 emu/g and 80 emu/g for FeCoNiMnAl and FeCoNiMnSn, respectively.[5]

Figure 3(b) shows *M-H* loops for three different discs cut from a slice of FeCoNiCrGa in Fig. 2(a). The saturation magnetization of 69 emu/g in sample 'A' including a big island region is approximately

TABLE II. A summary of EDS compositional analysis for each phase in HEAs (unit: atomic %).

HEA	Phase	Fe	Co	Ni	Cr	Ga	Al	Mn
FeCoNiCrGa	BCC	17	19	22	15	28	-	-
	FCC	21	22	18	20	18	-	-
	Δ	-4	-3	**+4**	-5	**+10**	-	-
	Island in sample A	93	4	1	0	2	-	-
FeCoNiCrAl	BCC	19	24	28	15	-	15	-
	FCC	24	26	22	20	-	8	-
	Δ	-5	-2	**+6**	-5	-	**+7**	-
FeCoNiCrMn	FCC	21	19	20	20	-	-	20

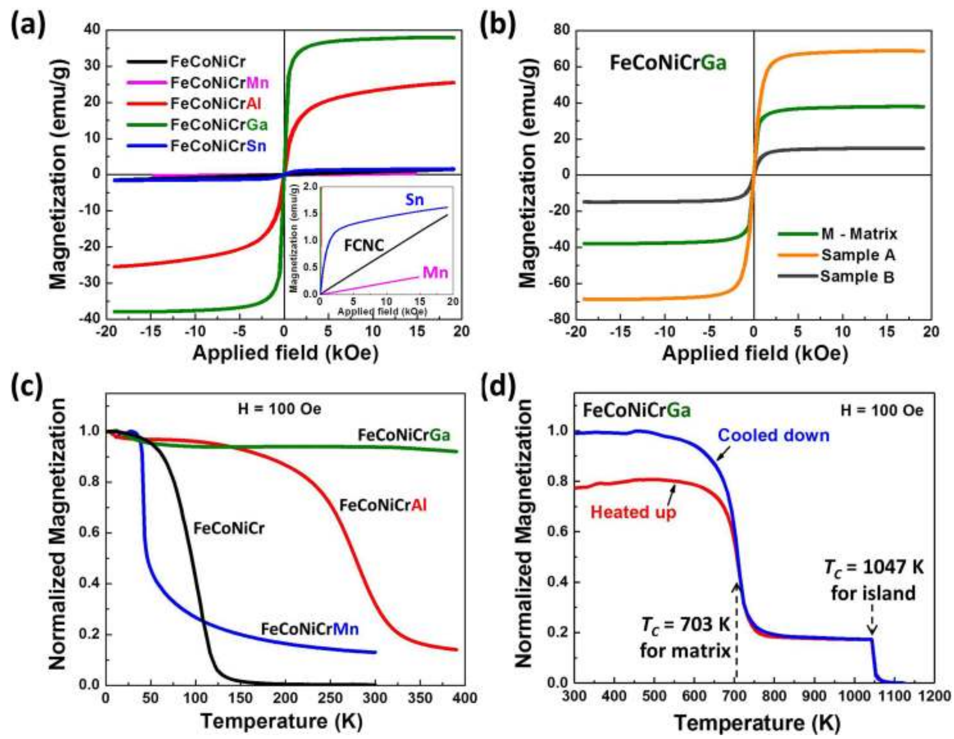

FIG. 3. Magnetic properties of the FeCoNiCr and FeCoNiCrX (X=Al, Ga, Mn and Sn) HEAs: (a) *M-H* curves measured at RT for the matrix of each HEA, (b) *M-H* curves measured at RT for the different samples of the FeCoNiCrGa HEA, (c) *M-T* curves at the temperature range of 2 K – 380 K for FeCoNiCr and FeCoNiCrX (X=Al, Ga and Mn), and (d) *M-T* curves at the temperature range of 303 K – 1123 K for sample 'A' of FeCoNiCrGa.

twice that of sample 'M' (matrix only) due to the high concentration of ferromagnetic Fe. In contrast, the saturation magnetization of 15 emu/g in sample 'B', which included a small island, is lower than that of sample 'M'. It is apparently reduced by a paramagnetic phase that corresponds to the small island. The magnetic property was verified by MPMS after removing the island from sample 'B'. Currently both islands are identified as magnetically different phases.

Figure 3(c) and 3(d) show the changes of Curie temperatures (T_C) obtained from the temperature dependence of magnetization (*M-T*) curves from 2 K up to 1123 K. For the FeCoNiCrMn HEA, T_C decreased even further from 104 K in FeCoNiCr to 41 K. It is not far from the simulated datum of 23 K for FeCoNiCrMn.[6] The RT paramagnetic FeCoNiCr alloy turned back to ferromagnetic by adding Al or Ga in an equiatomic composition, resulting in a significant increase of T_C to 277 K and 703 K, respectively. The T_C for FeCoNiCrGa could not be determined by the MPMS measurement as shown in Fig. 3(c) so the magnetization measurement at temperatures higher than 380 K was carried out in the VSM for sample 'A', where a magnetic field of 100 Oe was constantly applied to the sample. The sample was first heated up to 1123 K from RT, then cooled down to RT. From the results on structural and magnetic properties, we can expect that the sample 'A' contains two ferromagnetic phases. As expected, it was found that two drops occurred in magnetization, corresponding to the matrix (T_C = 703 K) and the island (T_C = 1047 K), respectively. The T_C for the matrix is higher than the point reported by Huang *et al.* (T_C = 649 K), and is rather close to the predicted T_C of 691 K by first-principle alloy theory.[12] On the other hand, the high T_C of 1047 K for the island is obviously reasonable for the dominant alloying components of 93% Fe and 4% Co, similar to T_C = 1043 K for pure Fe. The initial magnetization around RT increased by 25% after thermal cycling of RT-1123 K-RT. It might be due to a post-annealing effect on the stabilization of magnetic phases. It will be further studied by investigating the thermal effects on the magnetic properties of HEAs. Also, in order to understand the dramatic RT magnetic transition of ferro-para-ferro (FeCoNi-FeCoNiCr-FeCoNiCrX), it will be investigated for local magnetic and structural properties using

TABLE III. A summary of the relationship between *VEC* and crystal phases formed in FeCoNiCr-type and FeCoNiMn-type HEAs.[5–8,15–17]

	HEA	*VEC*	Predicted Phases	Actual Phases	*VEC* Agreement	M_S (emu/g)
FeCoNiCr-type	FeCoNiCr***Sn***	9.4	FCC	FCC	Yes	1.6
	FeCoNiCr***Ga***	9.2	FCC	BCC/FCC	No	38
	FeCoNiCr***Pd***	8.6	FCC	FCC	Yes	33
	FeCoNiCr***Mn***	8.0	FCC	FCC	Yes	0.5
	FeCoNiCr***Ti***	7.4	BCC/FCC	BCC/FCC	Yes	5
	FeCoNiCr***Al***	7.2	BCC/FCC	BCC/FCC	Yes	25
	FeCoNiCr$\boldsymbol{Al_2}$	6.5	BCC	BCC	Yes	11
FeCoNiMn-type	FeCoNiMn***Sn***	9.6	FCC	BCC	No	80
	FeCoNiMn***Ga***	9.4	FCC	BCC/FCC	No	80
	FeCoNiMn***Al***	7.4	BCC/FCC	BCC	No	148

Mössbauer spectroscopy and neutron scattering at the near future. The *M-T* curve for FeCoNiCrAl helps elucidate the paramagnetic behavior present in the positive slope of the *M-H* curve even at magnetic fields over 15 kOe (Fig. 3(a)). This is because the magnetic transition has already begun below room temperature resulting in mixed magnetic phases at RT. From these results on magnetic properties, the T_C and M_S at RT can be tailored by controlling the concentration of Al in FeCoNiCrAlx HEAs, which will be attractive for magneto-caloric effect (MCE) applications.

To evaluate the possibility of solid solution FCC and BCC phases in FeCoNiCrX HEAs, we introduced a parameter of valence electron concentration (*VEC*) which is the number of total electrons accommodated in the valence band including *s*-, *p*- and *d*-electrons.[13] The *VEC* was defined as $\Sigma^n{}_{i=1}$ $c_i(VEC)_i$, where $(VEC)_i$ is the *VEC* for the individual element, and c_i is the concentration of that element. It was observed that only the FCC phase exists at $VEC \geq 8.0$, a mixture of FCC and BCC exists at $6.87 \leq VEC < 8.0$, and solely the BCC phase at $VEC < 6.87$ in FeCoNi-based HEAs.[14] The proposed rule for solid solution formation by the *VEC* was well matched with our FeCoNiCr-type HEAs except for Ga addition. However, the FeCoNiMn-type HEAs (X=Al, Ga and Sn) that correspond to ferromagnetic materials with saturation magnetizations higher than 80 emu/g showed disagreement with the correlation, where the *VEC* of FeCoNiMn-type HEAs is shown in Table III.

IV. CONCLUSIONS

The dramatic change in magnetic transition from paramagnetism to ferromagnetism at RT was observed in high-entropy alloys (HEAs) when adding non-magnetic elements such as Al and Ga to a quaternary FeCoNiCr alloy with an FCC phase. This transition was associated with the coexistence of FCC and BCC phases and also manifested in an increase of saturation magnetization (M_S) and Curie temperature (T_C). The additions of Mn and Sn mostly retained the magnetic conditions of the paramagnetic FeCoNiCr alloy. The possibility of solid solution FCC and BCC phases in FeCoNiCr-type HEAs was well matched with the proposed rule for solid solution formation by the valence electron concentration (*VEC*), however the FeCoNiMn-type HEAs did not follow this trend. Among FeCoNiCr-type HEAs, the FeCoNiCrAl HEA is a good candidate for tailoring saturation magnetization and Curie temperature by controlling the concentration of Al.

ACKNOWLEDGMENTS

This work was supported by the U.S. Office of Naval Research (Code 321MS, Maritime Sensing). The authors would like to thank Dr. Hyunsoo Kim (University of Maryland, College Park) for his assistance with the MPMS measurements and Danielle Gerstner (Naval Surface Warfare Center, Carderock Division) for her assistance with the XRD measurements.

[1] J. W. Yeh, S. K. Chen, S. J. Lin, J. Y. Gan, T. S. Chin, T. T. Shun, C. H. Tsau, and S. Y. Chang, Advanced Engineering Materials **6**, 299 (2004).
[2] D. B. Miracle and O. N. Senkov, Acta Materialia **122**, 448 (2017).
[3] Z. Y. Sun, J. Zhang, J. B. Zhu, and J. C. Li, Arabian Journal for Science Engineering **39**, 8247 (2014).
[4] Y. F. Ye, Q. Wang, J. Lu, C. T. Liu, and Y. Yang, Materials Today **19**, 349 (2016).
[5] T. Zuo, M. C. Gao, L. Ouyang, X. Yang, Y. Cheng, R. Feng, S. Chen, P. K. Liaw, J. A. Hawk, and Y. Zhang, Acta Materialia **130**, 10 (2017).
[6] P. Li, A. Wang, and C. T. Liu, Intermetallics **87**, 21 (2017).
[7] F. Körmann, D. Ma, D. D. Belyea, M. S. Lucas, C. W. Miller, B. Grabowski, and M. H. F. Sluiter, Applied Physics Letters **107**, 142404 (2015).
[8] S. Huang, A. Vida, D. Molnar, K. Kadas, L. K. Varga, E. Holmstrom, and L. Vitos, Applied Physics Letters **107**, 251906 (2015).
[9] K. S. Lee, B. Bae, J.-H. Kang, K. R. Lim, and Y. S. Na, Materials Letters **198**, 81 (2017).
[10] S. Singh, N. Wanderka, K. Kiefer, K. Siemensmeyer, and J. Banhart, Ultramicroscopy **111**, 619 (2011).
[11] C. J. Tong, Y. L. Chen, S. K. Chen, J. W. Yeh, T. T. Shun, C. H. Tsau, S. J. Lin, and S. Y. Chang, Metallurgical Materials Transaction **36A**, 881 (2005).
[12] S. Huang, A. Vida, W. Li, D. Molnar, S. K. Kwon, E. Holmstrom, B. Varga, L. K. Varga, and L. Vitos, Applied Physics Letters **110**, 241902 (2017).
[13] U. Mizutani, *Hume-Rothery Rules for Structurally Complex Alloy Phases* (CRC Press, Boca Raton, 2011).
[14] S. Guo, C. Ng, J. Lu, and C. T. Liu, Journal of Applied Physics **109**, 103505 (2011).
[15] S. Huang, W. Li, X. Li, S. Schönecker, L. Bergqvist, E. Holmström, L. Károly, and L. Vitos, Materials and Designs **103**, 71 (2016).
[16] Y.-F. Kao, S.-K. Chen, T.-J. Chen, P.-C. Chu, J.-W. Yeh, and S.-J. Lin, Journal of Alloys and Compounds **509**, 1607 (2011).
[17] M. S. Lucas, L. Mauger, J. A. Muñoz, Y. Xiao, A. O. Sheets, S. L. Semiatin, J. Horwath, and Z. Turgut, Journal of Applied Physics **109**, 07E307 (2011).